

The effect of post-weld heat treatment on properties of low-alloyed CrMoNb steel after submerged welding

M. Gojić^{1*}, B. Mioč², L. Kosec³

¹*Faculty of Metallurgy, University of Zagreb, Aleja narodnih heroja 3, 44103 Sisak, Croatia*

²*Zlatna Aurora Ltd., Hrvatskoga narodnog preporoda 25, 44010 Sisak, Croatia*

³*Faculty of Natural Sciences and Engineering, University of Ljubljana, Aškerčeva 12, 1000 Ljubljana, Slovenia*

Received 2 August 2004, received in revised form 7 March 2006, accepted 8 March 2006

Abstract

The effect of post-weld heat treatment on mechanical properties, microstructure and fracture mode of low-alloyed CrMoNb steel was examined using an optical microscope, and a scanning and transmission electron microscopes. Steel plates, 18 mm thick, were welded by means of the submerged arc welding technique and then heat treated in the temperature range from 475 to 700 °C. It was found that the tensile strength, hardness and impact energy values decrease with the increasing annealing temperature, except for annealing at 550 °C and 625 °C. Anomalies were attributed to the precipitation of fine carbides. Complex cementite proved to be beneficial in controlling the fracture mechanism in impact (Charpy V-notch) and tensile tested specimens.

Key words: low-alloyed steel, welding, mechanical properties, microstructure, fracture surface

1. Introduction

Low-alloyed ferritic steels are attributed to the group of preferred materials showing suitable mechanical properties and high resistance to corrosion. Among them the low-alloyed CrMo steels are a popular variety of the steel family. They are widely used in the construction of pressure vessels, compressors, turbine rotors, power generating plants and other highly stressed construction components operating at elevated temperatures. They also serve in oil refineries and chemical industries as pipings, superheaters and tubular systems owing to the excellent creep and oxidation resistance properties [1].

The sufficient strength to withstand the inner pressure and the high toughness that can ensure safety against momentary impact due to unexpected accidents are the most critical requirements for the application of low-alloyed CrMo steels. It is generally known that the allowable stress of welded components is often based on their tensile strength and toughness. The manufacture of such components by welding can induce high residual stresses as well as microstructures

susceptible to cracking. In general, mechanical properties of the weld joints are inferior to those of the base metal [2]. Microstructural variations caused by welding are believed to be responsible for changes in mechanical properties of weld joints. For the low-alloyed CrMo steel weld joints a high percentage of service failures have been reported [3] to occur in the heat-affected zone (HAZ). The complex thermal cycling of the zone adjacent to the fusion line during welding tends to induce microstructural changes, and inhomogeneous HAZ may exhibit different mechanical properties.

Stress-relief cracking and reheat cracking of weldments may occur during stress-relief treatment or in high temperature service. Experimenting with the 1.25Cr-0.5Mo steel, Fujibashi et al. [4] have observed damage in the coarse-grained HAZ and weld metal. Higher residual stresses and brittle microstructure in the post-weld heat treatment (PWHT) conditions have been attributed to transverse weld metal cracking and multidirectional cracking in the coarse-grained zone rather than to service-induced stresses.

In weld joints or welded constructions brittle frac-

*Corresponding author: tel.: +385 44 5333 79, -80, -81; fax: +385 44 5333 78; e-mail address: gojic@siscia.simet.hr

Table 1. Chemical compositions of the base and weld metals (wt.%)

	Chemical composition										
	C	Mn	P	S	Si	Mo	Al	Cr	Ni	Cu	Nb
Base metal	0.07	1.40	0.016	0.003	0.46	0.45	0.04	1.42	0.49	0.09	0.06
Weld metal	0.09	1.43	0.012	0.003	0.62	0.47	0.03	1.19	0.14	0.08	0.015

ture can be induced under conditions of triaxial stress and high loading rate [2]. To reduce residual stress and increase toughness of the welds, PWHT must be performed immediately after welding, at temperatures below A_{c1} , i.e. before the transformation of ferrite into austenite takes place. Furthermore, the annealing process will improve the dimensional stability, enhance corrosion resistance and reduce hardness peaks in the weld joint area.

Our analysis of the changes in tensile strength behaviour and microstructure of the low-alloyed CrMoNb steel was aimed at establishing a relationship between those changes and the conditions of submerged arc welding (SAW) and annealing. Our objective was also to try to find a correlation between tensile strength, impact energy and fracture mode of the weld metal on the one hand, and microstructure on the other, with a view to assessing the effect of the PWHT temperature.

2. Experimental

Plates of 18 mm thickness, made from low-alloyed CrMoNb steel (Table 1), were welded using the SAW technique. The welding parameters are listed in Table 2. To ensure the quality of welds the weld edges were thoroughly cleaned. Preheating of weld edges was carried out at 190 °C. The weld root was obtained by means of the tungsten inert gas welding technique using a DCMS-IG solid electrode 2.4 mm in diameter. Fillet welding was carried out by the SAW technique using an S2CrMo1 BB25 flux-electrode with a 2 mm diameter. The weld joint had 18 passes. Interpass temperatures were carefully controlled to avoid weld cracking.

Immediately after welding the weld joint was subjected to heat treatment in the temperature range from 475 to 700 °C (± 3 °C) for 90 minutes, and was then air cooled.

Tensile testing was carried out in conformity with ASTM A-370 on both unwelded and welded specimens using an Instron tensile machine type 1196. The weld metal was positioned in the middle of the gauge measure. Tensile testing was done at room temperature.

Hardness was measured by the Vickers method at 30 kg load across the weld joint. Impact tests were performed on Charpy V-notch (CVN) specimens (10

Table 2. SAW parameters

Parameter	Value
Arc voltage (V)	29–30
Arc current (A)	270
Welding speed ($m \cdot min^{-1}$)	0.45

$\times 10 \times 55$ mm) at room temperature. V-notch was machined in the middle of the weld metal sample.

Sections of the weld joints 30 mm in length (cross-section 18×18 mm) with the weld metal in the middle part were cut from the welded plates and mechanically polished. The etchant used was 2% nital. The microstructure was examined using a light microscope (LM) and a scanning electron microscope (SEM) equipped with a unit for energy dispersive X-ray spectroscopy (EDX). Transmission electron microscopy (TEM) served to investigate the finer aspects of the microstructure that had not been revealed by SEM. Carbon extraction replicas were made to identify the carbide particles.

3. Results

Results of tensile testing for the base and weld metals, together with values of standard deviation are shown in Tables 3 and 4. The values are given as the means of three determinations. The tensile strength of the weld metal was higher than that of the base metal. The reduction in area for the base metal was high, about 64 %, it was lower for the weld metal (44.5 %), and it increased with a rise in the annealing temperature.

There was no scattering of the hardness values through weldment owing to the thermal history imposed by multipass welding. The welding coarsened HAZ formed from a previous pass could be affected by heat, like in the PWHT process. Hardness values across weldment are presented in Table 5. The hardness of the base metal after PWHT decreased with the increasing temperature, except when annealing took place at 625 °C. Also the hardness of the HAZ show local maxima at 550 °C. In the weld metal samples annealed at 475 °C hardness was 280 HV 30. As the

Table 3. Mechanical properties of the base and weld metals before PWHT. Tested at room temperature

	Yield strength (MPa)	Tensile strength (MPa)	Elongation (%)	Reduction of area (%)	Impact energy (J)
Base metal	800	923	16.0	64.0	40.5
Standard deviation	10.7	9.5	2.1	1.5	6.1
Weld metal	–	1059	–	44.5	27.3
Standard deviation		7.4		4.2	5.0

Table 4. Mechanical properties of the weld metal (WM) after PWHT at various temperatures. Specimens tested at room temperature

Temperature (°C)	Tensile strength (MPa)	Reduction of area (%)	Impact energy (J)
475	1036	47.8	43.0
Standard deviation	13.9	2.1	7.3
550	988	49.8	64.0
Standard deviation	16.8	4.1	6.1
625	998	49.7	49.0
Standard deviation	14.0	3.0	4.2
700	876	59.2	78.9
Standard deviation	18.2	1.8	5.4

Table 5. Hardness of weldment

	BM (HV 30)	HAZ (HV 30)	WM (HV 30)
Base metal	301	–	–
Standard deviation	6.2		
After welding	301	315	294
Standard deviation	5.3	6.4	3.5
After annealing at 475 °C	294	287	280
Standard deviation	4.7	3.8	5.0
After annealing at 550 °C	287	301	275
Standard deviation	5.4	3.1	5.2
After annealing at 625 °C	294	294	270
Standard deviation	5.9	4.5	4.1
After annealing at 700 °C	235	232	224
Standard deviation	4.1	3.1	3.0

annealing temperature rose up to 700 °C the hardness dropped to 224 HV 30.

The impact energy of the weld metal increased with the increasing annealing temperature except for annealing at 625 °C. The most likely reason for decreasing of the impact energy was of fine precipitates dispersed throughout the weld metal. The dispersed particles improve strength and reduce plasticity and toughness. Precipitated particles should be stronger than the matrix, adding strength through both their reinforcing action and the additional interfacial surfaces that present barriers to dislocation movement. The values of impact energy revealed that the microstructure of the weld metal was recovered at 700 °C.

The microstructure of the base metal consists of granular bainite (Fig. 1a). The bainite formed during continuous cooling of the CrMoNb steel differs from that expected to form during isothermal transformation. This was confirmed by the results of this study. Near the fusion line the HAZ consisted mainly of coarse-grained bainite (Fig. 1b). The region close to the fusion line experienced a peak temperature above A_{c4} (boundary between γ and $\gamma + \delta$ fields), and as a consequence, the prior austenite grain content increased. The weld metal consists of fine recrystallized ferrite grains characteristic for the upper bainite microstructure (Fig. 2a). Carbides were present on the boundaries of lath-like arrangements of ferrite and

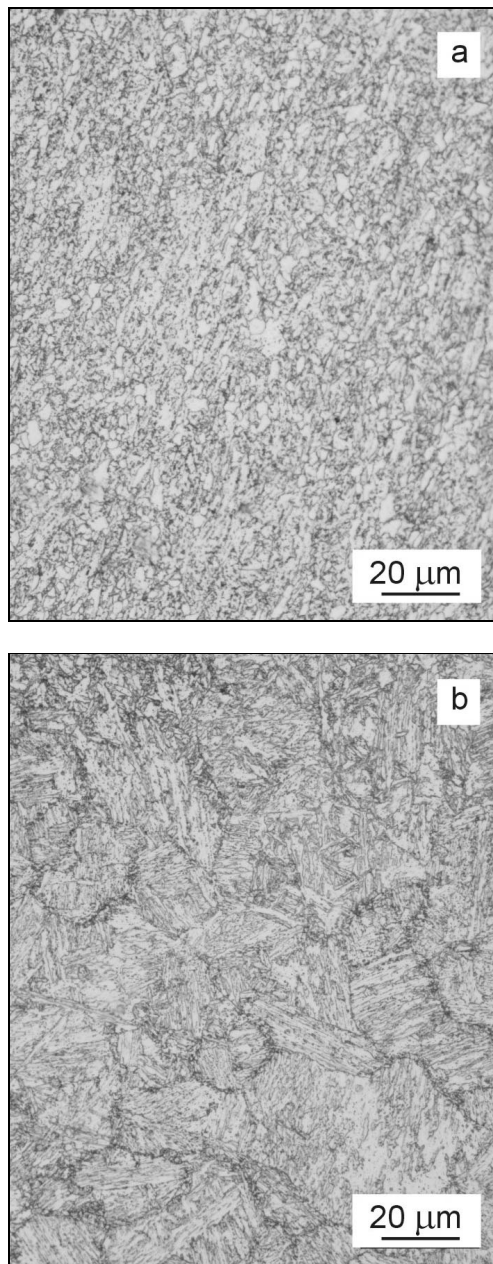


Fig. 1. Micrograph of the low-alloyed CrMoNb steel, LM, a) base metal, b) heat-affected zone/base metal interface.

prior austenite grains. This microstructural variation, clearly, was responsible for different hardness values across the weld joint (Table 5).

After PWHT a noticeable change in carbide distribution and morphology could be observed (Fig. 2b). Typical TEM-bright micrographs of the steel annealed at 700 °C, with visible rod-shaped carbides (20–50 nm), are shown in Fig. 3. In general, coarsening of microstructure of the weld joints as well as noticeable changes in the mechanical properties took place during PWHT.

In Fig. 4, facets of transgranular cleavage and areas

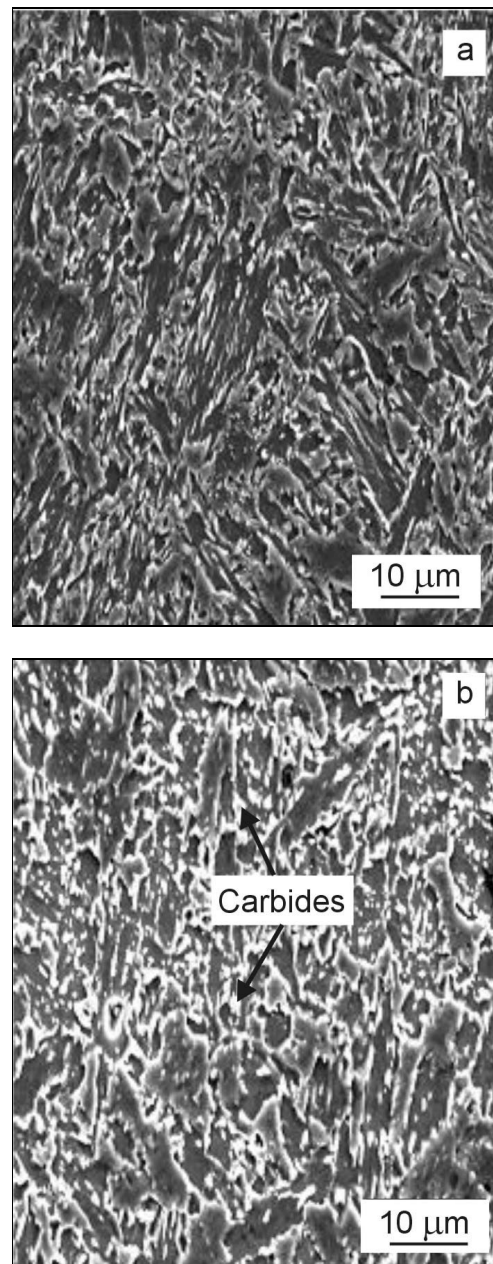


Fig. 2. SEM micrographs of low-alloyed CrMoNb steel weld metal, a) before PWHT, b) after PWHT.

of dimple morphology are illustrated. At the annealing temperature of 700 °C areas of dimple morphology were found in both CVN and tensile tested specimens (Figs. 5–7). Spherical carbide particles were found inside dimples. The EDX analysis demonstrated the presence of carbides and non-metallic inclusions at the fracture surfaces (Figs. 5b and 7b).

4. Discussion

During the thermal cycle the molten weld metal so-

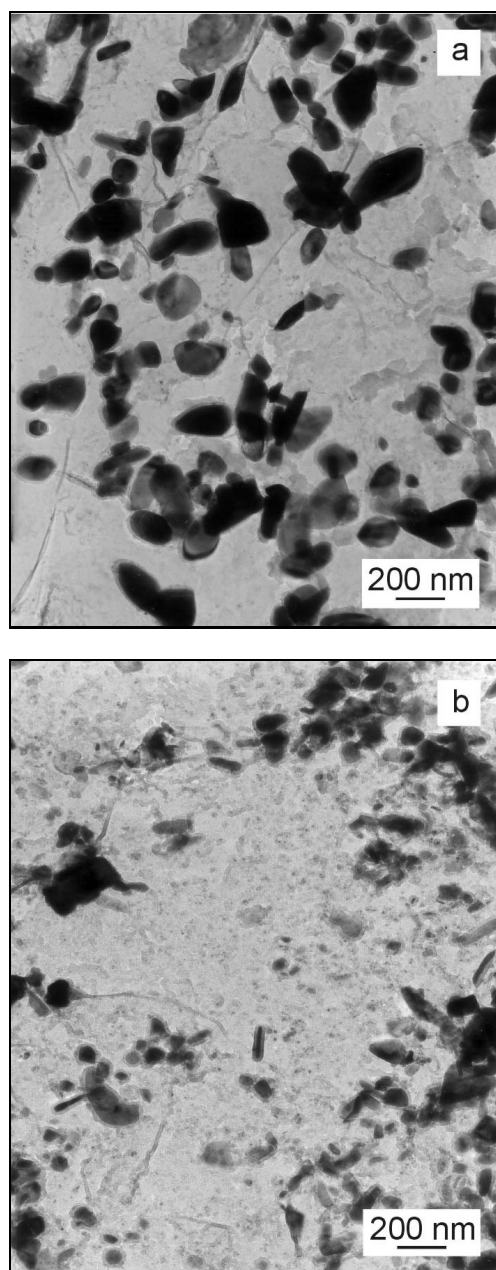


Fig. 3. Micrographs of low-alloyed CrMoNb steel weld metal, bright field images, TEM, a) I position, b) II position.

lidified in the form of austenite dendrites which were much smaller than the prior austenite grains of the normalized base metal [5]. A thorough mixing of alloying elements also took place in the liquid phase. The cooling rate of the weld metal was higher than that of the base metal. The resulting microstructures were much finer, and lent higher tensile strength to the weld metal as compared to the base metal (Table 3).

Hardness measurements yielded lower values for the weld metal. This could be accounted for by the chromium content of about 1.19 wt.%, which was

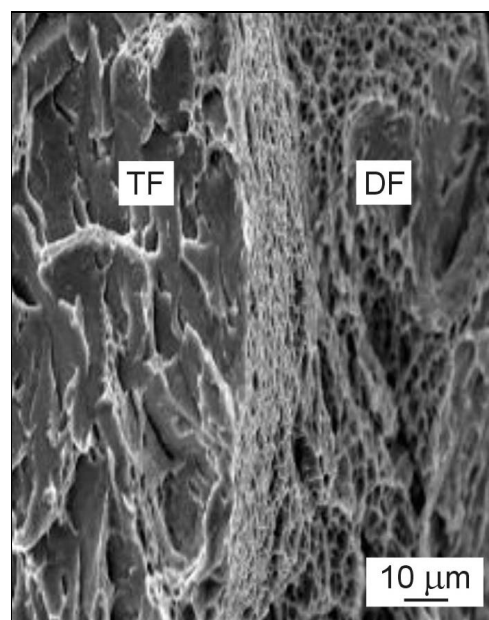


Fig. 4. SEM microfractograph of low-alloyed CrMoNb steel weld metal after Charpy impact testing. TF – transgranular cleavage, DF – areas of dimple morphology.

lower than the chromium content in the base metal (Table 1). The lower chromium content in the weld metal, and the absence of niobium, have been reported to diminish the hardenability of steel [6].

The chemical composition and/or microstructure of the weld metal as well as those of the HAZ are crucial to the mechanical properties of welded constructions. For weld joints of low-alloyed CrMoNb steel distinct microstructural variations, from the base metal to the weld metal through the HAZ, have been reported. Generally, changes within the HAZ are known to be intense and complex [7, 8]. The weld metal may have a cast microstructure, whereas the HAZ can be formed with ferrite, pearlite, bainite, martensite, or other components. The microstructure of HAZ is influenced with the peak temperatures experienced by different HAZ regions during the welding process [9].

The results obtained can be used for correlating the mechanical properties of the weld metal with the microstructures at various annealing temperatures (Table 4). At 625°C the weld metal was expected to have lower tensile strength than at 550°C. However, there was an increase in tensile strength at 625°C, which was accompanied by lower values of impact energy at room temperature. The phenomenon could be attributed to the microstructural changes, i.e. to the precipitation of fine carbides.

Similar trends in the precipitation of secondary phases during tempering have been reported in earlier studies on low-alloyed CrMo steels [10]. Higher hardness values at lower temperatures have been attributed to the conversion of ϵ carbide to cementite, to

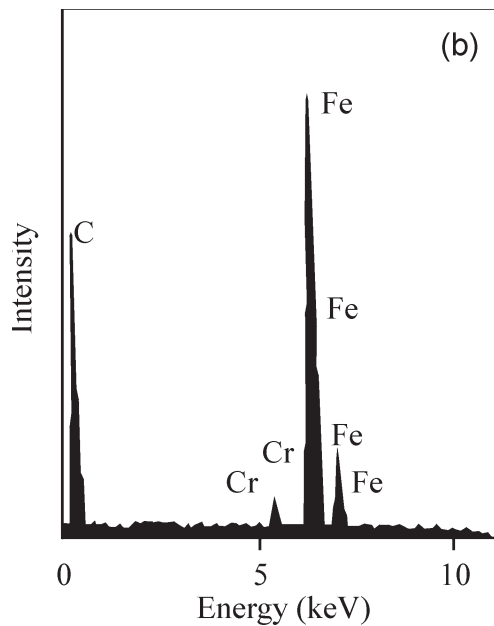
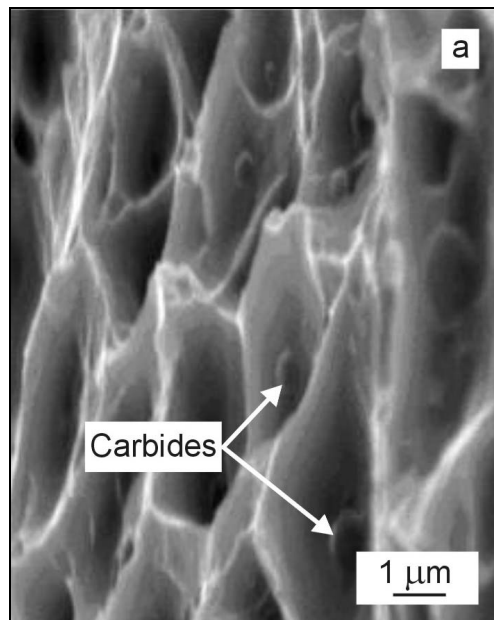


Fig. 5. SEM microfractograph of low-alloyed CrMoNb steel weld metal after Charpy impact testing (a) and EDX spectrum of carbide particle (b).

the precipitation of acicular M_2C carbides [11] and to the resistance of both carbides to the coarsening [12]. The carbide precipitation in the bainitic regions could be expected because of the increased carbon concentration in these regions due to the rejection of carbon into austenite [13].

The precipitation mechanism concerning low-alloyed CrMo steel welds is very complex, and is still not fully understood. According to the investigation of the secondary phase precipitation in CrMo and CrMoV steels by Janovec [14] the M_3C , M_7C_3 ,

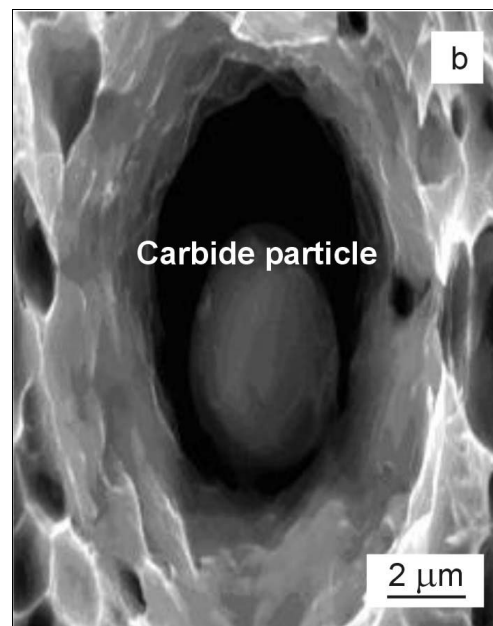
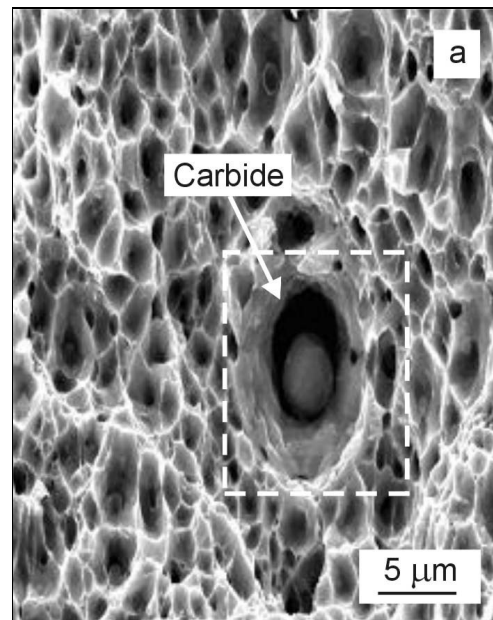


Fig. 6. SEM microfractographs of low-alloyed CrMoNb steel weld metal after tensile testing. Specimens annealed at 475 °C, a) basic view, b) detail.

M_2C and MC carbides are arranged in kinetic sequence, whereas $M_{23}C_6$ and M_6C carbides form separate areas in the time-temperature diagram. The first carbide to precipitate is cementite (M_3C), or some transient iron carbide, if the PWHT temperature is low. The precipitation sequence can be summarized as $M_3C \rightarrow M_7C_3 + M_2C + M_{23}C_6 \rightarrow M_{23}C_6 + M_6C$ [15]. Even if molybdenum is present in the investigated steel (Table 1), the precipitation of Mo-carbides was not established. Further studies are required before any conclusions concern-

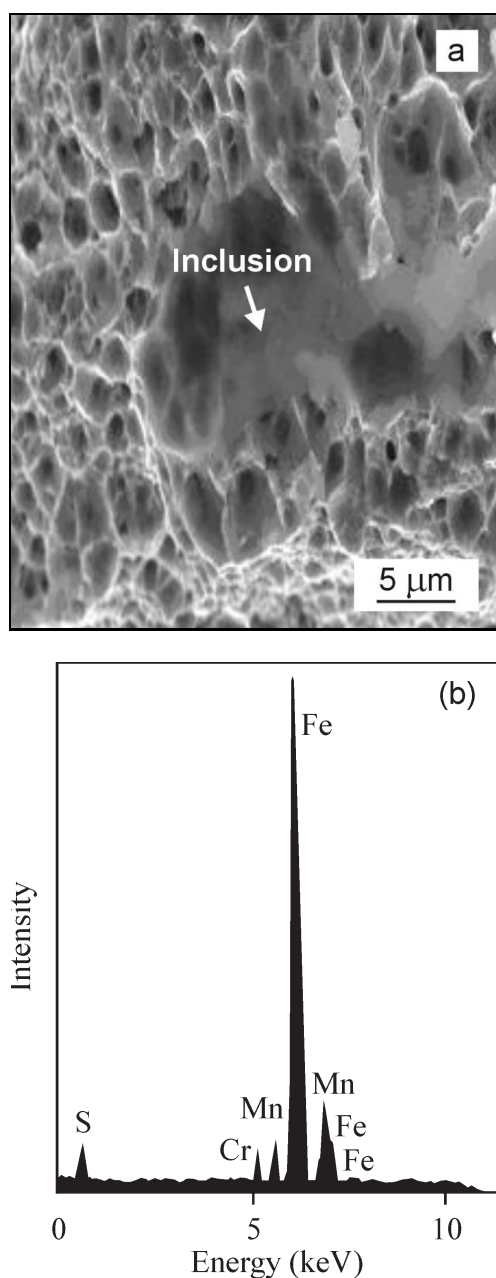


Fig. 7. SEM microfractograph of low-alloyed CrMoNb steel weld metal after tensile testing. a) Specimens annealed at 700 °C and b) EDX spectrum of non-metallic inclusion.

ing the precipitation mechanism in the steel can be drawn.

It is well known that fractography directly describes the fracture process and provides valuable evidence for the cause of failure. We investigated the fracture surfaces of the steel after CVN impact and tensile testing. Two distinct fracture modes were observed, facets of the transgranular cleavage (left side in Fig. 4) and the areas of dimple morphology (Fig. 4 – right side and Figs. 6, 7). Numerous spherical carbides were found to play a major role in controlling the

fracture mechanism. The beneficial effect of carbide particles on both the reduction in area and CVN impact energy can be attributed to the ductile fracture mode. The ductile fracture is characterized by nucleation, growth and coalescence of voids. The void nucleation is associated with the release of carbide particles from the ductile matrix on the steel plastic deformation. When the external load increases, growth and coalescence of voids are followed by microcrack formation, shear localization, and finally, by fracture of the loaded sample.

5. Conclusions

The results of investigation related to properties of low-alloyed CrMoNb steel before and after PWHT allow to draw the following conclusions:

1. The tensile strength of the weld metal was found to be higher than that of the base metal.

2. The HAZ microstructure consisted mainly of coarse-grained bainite near the fusion line, whereas the weld metal was characterized by the upper bainite microstructure.

3. EDX analysis confirmed the presence of complex cementite particles (M_3C) in the bainitic matrix.

4. Complex cementite was found to be present inside ductile dimples at fracture surfaces and was considered to have control over the fracture mechanism.

5. Changes in mechanical properties as a function of annealing temperature were directly related to the changes in the substructure and carbide distribution. After PWHT in the microstructure cementite particles are observed. Two anomalies were observed at 550 and 625 °C. It is likely due to the precipitation of fine carbide particles.

References

- [1] CHAUDHURI, S.—GHOSH, R. N.: *ISIJ Int.*, **38**, 1998, p. 881.
- [2] HRIVŇÁK, I.: *Theory of Weldability of Metals and Alloys*. Amsterdam, Elsevier 1992.
- [3] RAMAN, R. K. S.—GNONAMOORTHY, J. B.: *Corr. Sci.*, **34**, 1993, p. 1275.
- [4] FUJIBAYASHI, S.—ENDO, T.: *ISIJ Int.*, **42**, 2002, p. 1309.
- [5] DEGARMO, E. P.—BLACK, R. A.: *Materials and Processes in Manufacturing*. Hoboken, John Wiley & Sons, Inc. 2003.
- [6] GOJIĆ, M.—PRELOŠČAN, A.—MALINA, M.: *Metallurgija*, **30**, 1991, p. 161.
- [7] KURTHIK, V.—KASIVISWANATHAN, K. V.—LAHA, K.—RAJ, B.: *Weld. J.*, **84**, 2002, p. 265.
- [8] BOŠANSKÝ, J.—MAGULA, V.: *Acta Metall. Slovaca*, **10**, 2004, p. 352.
- [9] ADIL, G. K.—BHOLE, S. D.: *Can. Metall. Q.*, **31**, 1992, p. 151.

- [10] GOPE, N.—CHATTERJEE, A.—MUKHERJEE, T.—SARMA, D. S.: *Metall. Trans.*, 24A, 1993, p. 315.
- [11] BAKER, R. G.—NUTTING, J.: *J. Iron Steel Int.*, 192, 1959, p. 304.
- [12] SAROJA, S.—VIJAYALAKSHMI, M.—RAGHUNATHAN, V. S.: *J. Mat. Sci.*, 27, 1992, p. 2389.
- [13] THOMSON, R. C.—BHADESHIA, H. K. D. H.: *Mat. Sci. Tech.*, 10, 1994, p. 205.
- [14] JANOVEC, J.: In: *Proceedings of the 10th International Symposium on Metallography*. Ed.: Hrivňák, I. Košice, Department of Materials Science Faculty of Metallurgy TU Košice 1998, p. 102.
- [15] HRIVŇÁK, I.—SEMANOVÁ G.: In: *Proceedings of the 9th Symposium on Metallography*. Ed.: Hrivňák, I. Košice, Department of Materials Science, Faculty of Metallurgy TU Košice 1995, p. 371.